

## QUASAR CLUSTERING AT $25 h^{-1}$ kpc FROM A COMPLETE SAMPLE OF BINARIES<sup>1</sup>

ADAM D. MYERS<sup>2</sup>, GORDON T. RICHARDS<sup>3</sup>, ROBERT J. BRUNNER<sup>2,4</sup>, DONALD P. SCHNEIDER<sup>5</sup>, NATALIE E. STRAND<sup>6</sup>,  
PATRICK B. HALL<sup>7</sup>, JEFFREY A. BLOMQUIST<sup>3</sup>, AND DONALD G. YORK<sup>8</sup>

*ApJ*, in prep November 11, 2018

### ABSTRACT

We present spectroscopy of binary quasar candidates selected from Data Release 4 of the Sloan Digital Sky Survey (SDSS DR4) using Kernel Density Estimation (KDE). We present 27 new sets of observations, 10 of which are binary quasars, roughly doubling the number of known  $g < 21$  binaries with component separations of  $3'' \leq \Delta\theta < 6''$ . Only 3 of 49 spectroscopically identified objects are non-quasars, confirming that the quasar selection efficiency of the KDE technique is  $\sim 95\%$ . Several of our observed binaries are wide-separation lens candidates that merit additional higher-resolution observations. One interesting pair may be an M star binary, or an M star-binary quasar superposition. Our candidates are initially selected by UV-excess ( $u - g < 1$ ), but are otherwise selected irrespective of the relative colors of the quasar pair, and we thus use them to suggest optimal color similarity and photometric redshift approaches for targeting binary quasars, or projected quasar pairs. From a sample that is complete on proper scales of  $23.7 < R_{prop} < 29.7 h^{-1}$  kpc, we determine the projected quasar correlation function to be  $\overline{W}_p = 24.0 \pm_{10.8}^{16.9}$ , which is  $2\sigma$  lower than recent estimates. We argue that our low  $\overline{W}_p$  estimates may indicate redshift evolution in the quasar correlation function from  $z \sim 1.9$  to  $z \sim 1.4$  on scales of  $R_{prop} \sim 25 h^{-1}$  kpc. The size of this evolution broadly tracks quasar clustering on larger scales, consistent with merger-driven models of quasar origin. Although our sample alone is insufficient to detect evolution in quasar clustering on small scales, an  $i$ -selected DR6 KDE quasar catalog, which will contain several hundred  $z \lesssim 5$  binary quasars, could easily constrain any clustering evolution at  $R_{prop} \sim 25 h^{-1}$  kpc.

*Subject headings:* cosmology: observations — large-scale structure of universe — quasars: general — surveys

### 1. INTRODUCTION

Cosmologically, quasars can now be explained as one spectacular stage of an evolutionary process, initiated by gas-rich galaxy mergers, that ultimately helps redden elliptical galaxies (see, e.g., Hopkins et al. 2006, 2007a). That quasar activity might trace the early stages of merger-driven galaxy evolution makes quasar observations an essential ingredient in constraining galaxy formation scenarios. On the other hand, less luminous Active Galactic Nuclei (AGN), particularly at low redshift ( $z \lesssim 1$ ), may be better explained by less violent fueling mechanisms (e.g., Hopkins & Hernquist 2006) than the mergers that drive quasars' optical intensity. Given

that orientation can complementarily explain many differences between the AGN zoo (e.g., Antonucci 1993; Elvis 2000), new AGN constraints over a broad range of luminosity, particularly across  $z \sim 1$ , may be key to determining which elements of quasar behavior are mainly structural, and which are mainly evolutionary.

If quasars are associated with galaxy mergers, observations of binary quasars with proper separations comparable to the scale of small galaxy groups should offer interesting constraints. It has generally become accepted that most quasar pairs at similar redshifts that have image separations  $\gtrsim 3''$ , are binary quasars rather than lenses (Phinney & Blandford 1986; Bahcall et al. 1986; Kochanek et al. 1999; Rusin 2002; Oguri 2006). AGN activity can be exacerbated by tidal forces in galaxy mergers (Barnes & Hernquist 1996; Bahcall et al. 1997) and it has long been argued that this might explain an excess of binary quasars (Djorgovski 1991; Kochanek et al. 1999; Mortlock et al. 1999) and physical triples (Djorgovski et al. 2007). Hopkins et al. (2007b) suggest instead that a binary quasar excess simply reflects the increased probability for mergers to occur in regions that are overdense on small scales. If quasars form in mergers they will thus be naturally more biased at small scales. Hopkins et al. (2007b) further argue that orbits for which quasar activity might be exacerbated in both of two merging galaxies are prohibitively rare, even if few such events are needed to explain a binary quasar excess (Myers et al. 2007b; henceforth M07b).

The Sloan Digital Sky Survey (henceforth SDSS;

Electronic address: admyers@astro.uiuc.edu

<sup>1</sup> Some data presented here were obtained at Kitt Peak National Observatory, a division of the National Optical Astronomy Observatories, which is operated by the Association of Universities for Research in Astronomy, Inc. under cooperative agreement with the National Science Foundation.

<sup>2</sup> Department of Astronomy, University of Illinois at Urbana-Champaign, Urbana, IL 61801

<sup>3</sup> Department of Physics, Drexel University, 3141 Chestnut Street, Philadelphia, PA 19104

<sup>4</sup> National Center for Supercomputing Applications, Champaign, IL 61820

<sup>5</sup> Department of Astronomy and Astrophysics, 525 Davey Laboratory, Pennsylvania State University, University Park, PA 16802

<sup>6</sup> Department of Physics, University of Illinois at Urbana-Champaign, Urbana, IL 61801

<sup>7</sup> Department of Physics and Astronomy, York University, Toronto, ON M3J 1P3, Canada

<sup>8</sup> Department of Astronomy and Astrophysics, University of Chicago, Chicago, IL 60637

York et al. 2000) has renewed interest in binary quasars, and Hennawi et al. (2006; henceforth H06) have used SDSS data to categorically confirm earlier evidence (e.g., Djorgovski 1991; Hewett et al. 1998) that quasar clustering is enhanced on comoving scales  $\lesssim 100 h^{-1}$  kpc (proper scales of  $\lesssim 40 h^{-1}$  kpc at  $z \sim 1.5$ ). Binary quasars are scarce, with perhaps fewer than five hundred in the entire sky to  $g \lesssim 21$ , redshifts of  $z \lesssim 2.5$ , and comoving separations  $\lesssim 100 h^{-1}$  kpc (given the sample size in M07b). Deep, wide imaging, such as from the SDSS, is thus key to testing predictions of the nature of binary quasars; for instance, by studying quasar clustering as a function of redshift or luminosity. If enhanced small-scale quasar clustering is due to the enhanced bias of major galaxy mergers, rather than tidal forces exacerbating quasar activity, then there should be no redshift evolution in the relative bias of quasar clustering on large and small scales. Further, some merger-driven models predict stronger small-scale clustering for quasars than for lower-luminosity AGNs, due to different fueling mechanisms (e.g., Hopkins et al. 2007b).

Binary quasar samples are typically assembled from pairs that are initially targeted as possible gravitational lenses (e.g., Mortlock et al. 1999; H06). Because of this, the two members of most known binary quasars have similar colors. Although color similarity may be optimal in detecting lenses, scatter in the quasar color-redshift relation (e.g., Richards et al. 2001) dictates that strict color similarity cannot select *all* binary quasars. As binary quasars are useful in testing merger-driven models of quasar activity, it is disconcerting that color similarity cuts might discard particularly informative binaries, such as any that are being exacerbated by tidal forces in merging galaxies. Further, as binary quasars are scarce, relaxing color criterion might help provide enough binaries to study their redshift evolution.

We have now performed spectroscopy of a sample drawn from a complete, UVX ( $u - g < 1$ ) set of SDSS Data Release 4 (henceforth DR4; Adelman-McCarthy et al. 2006) binary quasar candidates (see Table 1 of M07b). The sample,  $\sim 45\%$  of which has now been identified, is photometrically selected using the Kernel Density Estimation (KDE) technique of Richards et al. (2004). Our aim is to compile an extensive, homogeneous set of binary quasars, with proper separations  $\lesssim 40 h^{-1}$  kpc, mainly to study quasar clustering on small scales, ultimately as a function of redshift. Most of our binary candidates are unlikely to be observed in the main SDSS quasar survey (e.g., Schneider et al. 2007), because our observations probe fainter, and because SDSS fibers (in single tiles) cannot be placed closer than  $55''$ . Our approach differs from previous studies of binary quasars. In particular, our main goal is to study binary quasars, not gravitational lenses (unlike the samples compiled in, e.g., Kochanek et al. 1999; Mortlock et al. 1999; H06). Thus, excepting our initial UVX cut, our binaries are the first sample selected regardless of the relative colors of the component quasars. This allows an investigation of whether color similarity can be used to optimally target binary quasars (§3).

In §2, we discuss our initial results in compiling a homogeneous, spectroscopic binary quasar sample from the SDSS, and report 27 sets of new observations of binary

quasar candidates. In §4 we use a subset of these observations to present the first analysis of quasar clustering on small scales using a *complete* spectroscopic sample of binary quasars. All our binaries are selected from the DR4 KDE candidates of M07b, and are therefore a straightforward subset of SDSS DR4, making our selection function very simple. We correct all magnitudes for Galactic extinction using the maps of Schlegel, Finkbeiner & Davis (1998), unless otherwise noted. We adopt  $\Omega_m = 0.27$ ,  $\Omega_\Lambda = 0.73$ , consistent with WMAP3 (Spergel et al. 2007), and  $h \equiv H_0/100 \text{ km s}^{-1} \text{ Mpc}^{-1} = 0.7$ . We denote transverse proper (comoving) scales as  $R_{prop}$  ( $R$ ) and radial proper (comoving) scales as  $s_{prop}$  ( $s$ ).

## 2. DATA

### 2.1. Observations

#### 2.1.1. Candidate Selection

Our candidate binary quasars are photometric objects in SDSS DR4 that are classified as quasars by the KDE technique (Richards et al. 2004), have  $u - g < 1$ ,  $g < 21$ , and are within  $3''$  to  $6''$  of another such object. The SDSS *ugriz* filters are described in Fukugita et al. (1996). As in M07b, we inspect our candidates and discard any that are clearly not quasars (close KDE candidates are occasionally misclassified H II regions in low-redshift galaxies). We restrict our spectroscopy, and analysis, to quasar pairs with angular separations of  $\Delta\theta > 3''$ , so that components of a pair appear clearly separated in SDSS imaging (e.g., H06). Although scales that are comparable to small galaxy groups or smaller are most useful in testing merger models of quasar activity, our upper limit of  $\Delta\theta < 6''$  is somewhat arbitrary, providing a reasonable number of candidates for a small spectroscopic study. Table 1 of M07b lists our 98 DR4 candidate binaries (and a further 13 candidates with  $\Delta\theta < 3''$ ). At  $g < 21$  the KDE technique, coupled with a UVX ( $u - g < 1$ ) cut, selects quasars with 95% efficiency, and is over 95% complete for redshifts of  $0.2 \lesssim z \lesssim 2.4$  (e.g., Richards et al. 2004; Myers et al. 2006, 2007a). Our survey goal is an efficiently classified, statistical, sample of binary quasars, which are UVX but are otherwise selected irrespective of the relative colors of the components of the binary. At  $z \lesssim 2.5$ , our selection should thus only bias our sample against those binaries where one or both component quasars is reddened beyond  $u - g = 1$ .

#### 2.1.2. Spectroscopy

Spectroscopy of our DR4 KDE binary quasar candidates was obtained with the R-C Spectrograph on the Mayall 4-m, over 5 nights (UT 2007 February 22–26) at Kitt Peak National Observatory. We used a  $1.5''$  by  $98''$  long-slit set at the position angle of the candidate binary, allowing both components to be simultaneously observed. The KPC-10A grating and WG360 blocking filter yielded a resolution of  $\sim 5\text{\AA}$  and a wavelength coverage of  $\sim 3800\text{--}7500\text{\AA}$ . The most useful observations were obtained on February 25 and 26, due to cloud and wind on other nights. Over February 25 and 26, the seeing was  $\lesssim 1.5''$ , allowing even our closest binary candidates ( $\sim 3''$ ) to be spatially separated. The survey goals were a positive identification and redshift for each DR4 KDE binary candidate. This typically required a 15 minute

exposure when the *faintest* member of the candidate binary was at  $g \sim 19.5$  and three 20 minute exposures (or longer) for  $g \sim 21$ , although the  $\gtrsim 70\%$  illuminated Moon on February 25 and 26 typically prevented our  $g \sim 21$  candidates from being spectroscopically identified.

Spectra were reduced at the telescope, using IRAF<sup>9</sup>. Exposures ceased once a binary candidate could be identified as; (1) containing one star or galaxy; or (2) containing two quasars with established redshifts. We estimate redshifts using the rest frame emission wavelengths listed in Table 2 of Vanden Berk et al. (2001). Based on deriving redshifts, where possible, from several different lines in each quasar’s spectrum, our typical error is  $\Delta z \sim 0.0031$ . A similar approach suggests a mean velocity precision of  $\sim 370 \text{ km s}^{-1}$ , with little redshift dependence. We note that this is likely an overestimate, as velocity differences between quasars are usually found to be more precise when cross-correlating the full spectra, rather than measuring line shifts (e.g., Tonry & Davis 1979; Djorgovski & Spinrad 1984).

Tables 1a–1d detail our new observations. Table 1a lists objects for which we obtained an identification for only one member of the candidate binary. Table 1b lists confirmed binary quasars. Following H06, we classify quasar pairs with a line-of-sight velocity difference of  $|\Delta v_{\parallel}| < 2000 \text{ km s}^{-1}$  ( $s_{prop} < 9.5 \text{ h}^{-1} \text{ Mpc}$  at  $\bar{z} = 1.4$ ) as a binary. Table 1c lists DR4 KDE binary candidates that are actually “projected” quasar pairs (with components that lie at different redshifts), or pairs in which one object is not a quasar. When both redshifts listed in Table 1c have some uncertainty, a binary quasar interpretation can still be ruled out, based on strong lines observed in both quasars but at discrepant wavelengths. Pairs that are harder to definitively identify are listed in Table 1d (see §2.2.2).

In all, we spectroscopically identified 49 objects, mainly in areas with Galactic absorption  $A_g \lesssim 0.17$ . Of these identified objects, 44 are both members of 22 candidate quasar pairs, and 5 are objects from pairs for which we identified only one member. Of the 49 identified objects 46 are quasars, confirming the KDE technique is  $\sim 95\%$  efficient for  $A_g \lesssim 0.21$  (Myers et al. 2007a). Of the 22 candidate quasar pairs for which we identified both components, 3 are quasar-non-quasar pairs, 9 are projected quasar pairs (i.e. at disjoint redshifts), and 10 are binary quasars. Several of the 10 binary quasars could, in fact, be previously unrecorded lenses; see §2.2.1). In Table 2 we list previously known quasar pairs that also meet the criteria to be included in our DR4 KDE binary candidate sample. Previously known candidates include 12 non-binaries, 9 binaries, and 2 lenses. Approximately half of the 98 ( $3'' \leq \Delta\theta < 6''$ ) DR4 KDE candidates have now been spectroscopically identified (see Table 3). With the caveat that bright objects may have been observed first,  $\sim 42\%$  of the candidate pairs are binary quasars, and only  $\sim 16\%$  of the pairs contain a non-quasar.

## 2.2. Interesting Spectroscopic Pairs

<sup>9</sup> Distributed by the National Optical Astronomy Observatory, which is operated by the Association of Universities for Research in Astronomy, Inc., under cooperative agreement with the National Science Foundation.

### 2.2.1. Potential Lenses

Five pairs in Table 1b have sufficiently similar spectra, at our  $\sim 5\text{\AA}$  resolution, that they might be a lensed quasar rather than a binary. As lenses with image separations in the range  $3'' \leq \Delta\theta < 6''$  are rare (e.g., Inada et al. 2007), particularly for  $z \lesssim 2$ , we interpret these objects as binaries (see also Kochanek et al. 1999), although they certainly merit higher-resolution spectroscopy. A lensing interpretation is especially unlikely for the three possible lenses used in our clustering analysis (§4), which have  $\sim 5''$  separations and, in two cases, dissimilar colors. In Figure 1 we display the spectra of our most likely lens candidates. SDSSJ1158+1235A and B, in particular, have almost identical spectra at our resolution.

### 2.2.2. Notes on Ambiguous Binaries

Table 1d, lists four candidates that we could not definitively identify. We conclude that two of these objects are binaries, for the following reasons, quoting all wavelengths in the observed frame.

SDSSJ093424.32+421130.8 and SDSSJ093424.11+421135.0 consist of a quasar at  $z = 1.339$  and a featureless spectrum (after 4200s of exposure). SDSSJ093424.11+421135.0 is faint (observed  $g = 21.01$ ), probably a star, and has no obvious emission near  $4460\text{\AA}$  or  $6550\text{\AA}$ , the principal emission lines used to identify SDSSJ093424.32+421130.8. We therefore conservatively conclude that this is not a binary quasar.

SDSSJ120727.09+140817.1 and SDSSJ120727.25+140820.3 both have ambiguous redshifts. The fainter object (observed  $g = 20.39$ ) has broad emission at  $4320\text{\AA}$ , and near  $7840\text{\AA}$  at the red edge of our coverage. Although the brighter object ( $g = 20.27$ ), has possible, low signal-to-noise ratio, emission near  $4340\text{\AA}$  we discount it based on the  $4320\text{\AA}$  emission in the fainter object being strong, and that the objects are, obviously, observed under similar conditions. We tentatively conclude that this pair is not a binary quasar.

SDSSJ1235+6836A,B (see Figure 2) are an interesting pair with highly dissimilar colors. SDSSJ1235+6836B is apparently a quasar with significant broad emission near  $3895\text{\AA}$  and  $7050\text{\AA}$  and weaker emission near  $4790\text{\AA}$ . SDSSJ1235+6836A is most likely a quasar, with probable broad emission near  $3910\text{\AA}$  and possible emission near  $4820\text{\AA}$ , lying behind a classic M star observed at the red end of the spectrum. As  $\lesssim 3900\text{\AA}$ , is near the blue edge of our coverage, an alternative possibility is that one or both objects are just M stars with very strong, blended Ca II H and K emission. Assuming the proper motion of the M star(s) is moderate, this object may look more or less like an M star-quasar pair over time.

SDSSJ1507+2903A,B have strong emission near  $5250\text{\AA}$  and  $5215\text{\AA}$ , respectively. Neither spectrum has additional features over  $3800\text{--}7500\text{\AA}$ , and so we assume that the emission is Mg II, placing both quasars at  $z \sim 0.87$ . The ambiguity for this pair is that their redshifts imply  $|\Delta v_{\parallel}| = 2100 \text{ km s}^{-1}$ . As a shift of  $\delta z < 0.0005$ , far smaller than our typical precision, can bring these quasars within  $|\Delta v_{\parallel}| < 2000 \text{ km s}^{-1}$ , we identify this pair as a binary.

### 3. COLOR SELECTION OF BINARY QUASARS

To study relative color selection of binary quasars, we use the  $\chi^2$  color similarity statistic introduced by H06

$$\chi_{color}^2(A) = \sum_{\text{ugriz}} \frac{(f_2^i - Af_1^i)^2}{[\sigma_2^i]^2 + A^2[\sigma_1^i]^2} \quad (1)$$

where the subscripts 1 and 2 represent the components of a pair. The superscript  $i$  refers to flux ( $f$ ) in the 5 SDSS bands ( $ugriz$ ). For *asinh* magnitudes ( $m$ )

$$f^i = 2F_0 b^i \sinh[-m^i/P - \ln b^i] \\ \sigma_f^i = (\sigma_m^i/P) \sqrt{(2F_0 b^i)^2 + (f^i)^2} \quad (2)$$

where  $P = 2.5/\ln 10$  (Pogson 1856),  $F_0 = 3630.78\text{Jy}$ , and  $b^{[u,g,r,i,z]} = [1.4, 0.9, 1.2, 1.8, 7.4] \times 10^{-10}$  (Lupton et al. 1999; Stoughton et al. 2002). A quasar pair with more similar colors has a lower  $\chi_{color}^2$ . Iterative equations for calculating  $A$  in Equation 1 can be ill-conditioned for  $\chi_{color}^2 \gtrsim 30$ , so, throughout this work, we numerically determine  $A$  by bisection.

Binary quasars are often pairs rejected from gravitational lens searches, and as such, the components of known binaries typically have very similar colors, a long-known example being SDSSJ1637+2636A,B ( $\chi_{color}^2 = 2.8$ ; see Table 2; Sramek & Weedman 1978; Djorgovski & Spinrad 1984). Schemes designed to optimize binary quasar searches by selecting pairs with similar colors, will, therefore, naturally reselect known binary quasars. Our DR4 KDE objects are simply all candidates with a high probability of being quasars and thus, after the initial homogeneous UVX cut, are selected irrespective of the *relative* colors of the components of the pair. The UVX cut itself, at  $z \lesssim 2.5$ , should only bias our sample against those binaries with a component that is intrinsically dust-reddened beyond  $u - g = 1$ . Our sample should thus be useful in determining color similarity cuts to optimize binary quasar selection. However, some of the quasar pairs in Table 2 were selected by H06 to have  $\chi_{color}^2 < 20$ ; as we avoided reobserving these pairs, our data in Tables 1b–1d may be biased to  $\chi_{color}^2 > 20$ .

In the upper-left panel of Figure 3, we demonstrate that the  $\chi_{color}^2$  values of the DR4 KDE binary candidates identified to date fairly represent the full sample. We compare the cumulative fraction of the 45 identified candidates (i.e., Table 3) to the remaining 53 ( $3'' < \Delta\theta < 6''$ ) candidates, as a function of  $\chi_{color}^2$ . A two-sample Kolmogorov-Smirnov test cannot distinguish the distributions, suggesting that the colors of the observed candidates fairly represent all candidates. The upper-right panel of Figure 3 compares the  $\chi_{color}^2$  cumulative probability for the 21 confirmed binary quasars (or lenses) and the 24 confirmed non-binaries (projected quasar pairs, star-quasar pairs, NELG-quasar pairs). The K-S test probability that these two distributions are drawn from the same underlying  $\chi_{color}^2$  distribution is  $\sim 10\%$ , suggesting that  $\chi_{color}^2$  can indeed discriminate binary quasars from non-binaries.

As our candidates are selected without a  $\chi_{color}^2$  cut, we can ask what  $\chi_{color}^2$  limit optimizes completeness (number of binaries/21 total binaries) and efficiency (num-

ber of binaries/45 observed candidates). To sample  $\gtrsim 50\%$  ( $\gtrsim 66\%$ ) of binary quasars requires  $\chi_{color}^2 \lesssim 10$  ( $\chi_{color}^2 \lesssim 20$ ), efficient at 70% (55%), while  $\chi_{color}^2 \lesssim 70$ –100, contains 95% of all binaries (only missing the “ambiguous” SDSSJ1235+6836A,B) and remains 50% efficient. A  $\chi_{color}^2 < 70$  cut rejects all but one quasar-star pair, while retaining all quasar-quasar projections.

As there is reasonable scatter in the quasar color-redshift relation (e.g., Richards et al. 2001) full photometric redshift (henceforth *photoz*) information should better select binary quasars. To test this, we consider the primary “CZR” *photoz* solution (Weinstein et al. 2004; “ $z_{phot}$  range” in Tables 1–2) for each quasar in our sample. We determine the overlap fraction of the primary *photoz* solutions of the two quasars in a pair, multiplying by the probability that the quasar occupies that primary peak.

The completeness and efficiency of a binary quasar sample obtained by considering *photoz* overlap are plotted in the lower-left panel of Figure 3. Confirmed non-binaries typically have no *photoz* overlap. A probability cut at  $> 3\%$  overlap will return 90% of binaries and is 73% efficient. The two binaries that are missed are the “ambiguous” SDSSJ1235+6836A,B, and SDSSJ1637+2636A,B, the “A” component of which has a poorly behaved *photoz* solution. If one additionally observed all candidates that contained a quasar with a poor *photoz* (characterized by a probability of  $< 0.5$ ), 95% of binary quasars would be observed at 69% efficiency. Of course, although cutting on *photoz* overlap is a more efficient mechanism for selecting binaries, it does so at the expense of projected quasar pairs. A cut at  $< 3\%$  overlap could therefore be used to discard binary quasars in favor of projected pairs.

In conclusion, if a survey’s goal is to select both binary quasars and projected quasar pairs, a cut of  $\chi_{color}^2 \lesssim 70$  (after first applying an efficient photometric quasar classification technique such as KDE) will return 97% of binaries, lenses and projected pairs (multiplied by, e.g., the 95% completeness of the KDE technique itself), at 93% efficiency. This is hardly surprising, and simply further confirms that the KDE technique is  $\sim 95\%$  efficient (Richards et al. 2004; Myers et al. 2006, 2007a). Cuts of  $\chi_{color}^2 \lesssim 20$ , or stricter, may be necessary without prior KDE photometric classification but will miss  $\gtrsim 33\%$  of all binary quasars. Interestingly, 2 ( $\sim 10\%$ ) of the DR4 KDE binary quasars (and one lens!) have more dissimilar colors than any of the quasar-quasar projections, hinting that physical interactions may affect the colors of a few binary quasars. If a survey goal is observing only binary quasars, a cut of  $> 0.03$  in the overlap of the two quasars’ *photozs* is superior to  $\chi_{color}^2$  selection. We stress that this analysis applies only to quasars pre-selected using an efficient photometric classification technique.

### 4. PROJECTED QUASAR CLUSTERING AT 25 $h^{-1}$ kpc

With our new observations (Table 1b and 1d), we have now identified all DR4 KDE binary quasar candidates with  $A_g < 0.17$ ,  $g < 20.85$  and  $3.9'' < \Delta\theta < 5.2''$ . In Table 4 we compile the binaries that meet these criteria. The three possible lenses in this subsample are wide-separation ( $\Delta\theta \geq 4.5''$ ), making them likely binaries. As our sample is complete over  $3.9'' < \Delta\theta < 5.2''$ , it is also

effectively complete for quasars in SDSS DR4 with separations on proper scales of  $23.7 < R_{prop} < 29.7 h^{-1}$  kpc over  $1.0 < z < 2.1$ .

We study quasar clustering using the  $DD/DR$  estimator (e.g., Shanks et al. 1983) for quasar-quasar ( $QQ$ ) pair counts compared to expected quasar-random ( $QR$ ) pair counts

$$\overline{W}_p = \frac{QQ}{\langle QR \rangle} - 1 \quad (3)$$

Higher-order corrections (e.g., Landy & Szalay 1993), reduce to Equation 3 for the small scales and large volumes we consider. We use small-number Poisson errors from Gehrels (1986). Poisson errors are valid on small scales where pair counts are independent (e.g., Croom & Shanks 1996; Myers et al. 2006).

As our clustering sample is a subset of all SDSS DR4 photometric objects, our selection function is very simple. We calculate  $\langle QR \rangle$  in Equation 3 by constructing a catalog of random points with the same angular coverage as SDSS DR4, correcting the SDSS data for mask holes, as in Myers et al. (2006, 2007a). We further limit our random catalog to areas of the sky with Galactic absorption  $A_g < 0.17$ . We assign random points a redshift according to a fit to the normalized redshift distribution of ( $A_g < 0.17$ ,  $g < 20.85$ ) quasars in the DR1 catalog (Schneider et al. 2003), from which the DR4 KDE quasar classification is trained. Figure 7 of Myers et al. (2006) is similar to this redshift distribution, and Myers et al. (2006) argue that including additional quasars that overlap the KDE color space minimally impacts this  $N(z)$  distribution. To represent our fit, we use a modified Gaussian

$$dN = \beta \exp \frac{-|z - \bar{z}|^n}{n\sigma_i^n} dz \quad (4)$$

and find a best fit with  $\bar{z} = 1.4$ ,  $\sigma = 0.6$ ,  $\beta = 0.65$  and  $n = 3$  (see also Myers et al. 2007a). We have repeated our analyses instead using a spline fit, and our results differ by  $\lesssim 2\%$ .

To determine  $\langle QR \rangle$  in a given bin we use a random catalog with 1000 times as many points as the ( $A_g < 0.17$ ,  $g < 20.85$ ) KDE DR4 photometric quasar catalog. We total all  $QR$  counts in the *angular* bin of interest, and normalize the result (divide by 1000). We then create a random catalog with points distributed according to Equation 4, and determine the fraction of pairs that would lie within  $|\Delta v_{\parallel}| < 2000 \text{ km s}^{-1}$  by Monte Carlo sampling to 0.1% precision. Multiplying this fraction by the normalized  $QR$  counts yields  $\langle QR \rangle$ . In a bin of  $3.9'' < \Delta\theta < 5.2''$  we expect 30.3  $QR$  counts. Over our full  $N(z)$ , we expect 0.0166 pairs with  $|\Delta v_{\parallel}| < 2000 \text{ km s}^{-1}$ . Thus  $\langle QR \rangle = 0.503$ , compared to  $QQ = 16$  for the 8 (non-unique) pairs in Table 4. The implied projected correlation function averaged over  $3.9'' < \Delta\theta < 5.2''$  is thus  $\overline{W}_p = 30.8 \pm_{11.0}^{15.7}$ . We note that, for all candidate pairs,  $QQ(3.9'' < \theta < 5.2'') = 40$ , yielding an angular correlation of  $\omega(\theta) = (40/30.3) - 1 = 0.320 \pm_{0.292}^{0.366}$ , consistent with M07b.

One of the pairs (SDSSJ1507+2903) in Table 4 has  $|\Delta v_{\parallel}| < 2100 \text{ km s}^{-1}$ . We reasonably include this pair

in our analysis, given the precision of our redshift estimates. Instead rejecting SDSSJ1507+2903 and assuming  $QQ = 14$  would lower our estimate of  $\overline{W}_p$  by  $\sim 10\%$ . The  $|\Delta v_{\parallel}| < 2000 \text{ km s}^{-1}$  limit from H06 is intended to bracket possible shifts in quasar lines, and thus incorporate possible errors on  $|\Delta v_{\parallel}|$  but is otherwise arbitrary. Although our Monte Carlo sampling of  $|\Delta v_{\parallel}| < 2000 \text{ km s}^{-1}$  pairs does not model any error in  $|\Delta v_{\parallel}|$ , relaxing this velocity window to  $|\Delta v_{\parallel}| < 2100 \text{ km s}^{-1}$  would imply  $\langle QR \rangle = 0.533$  for  $QQ = 16$ , lowering our  $\overline{W}_p$  estimate by  $\sim 5\%$ . As the change in  $\overline{W}_p$  implied by relaxing our velocity criterion is far smaller than our errors on  $\overline{W}_p$ , we proceed including SDSSJ1507+2903 in our analyses and maintaining  $|\Delta v_{\parallel}| < 2000 \text{ km s}^{-1}$  in our Monte Carlo sampling.

We apply our approach to different redshift ranges by weighting the number density of points in the initial calculation of  $QR$  by the relative fraction of DR4 KDE quasars obtained by integrating under Equation 4. We can thus determine  $\langle QR \rangle$  over  $1.0 < z < 2.1$ , for which our sample is spatially complete on scales of  $23.7 < R_{prop} < 29.7 h^{-1}$  kpc. In Figure 4 we compare the small-scale clustering of quasars determined from our complete DR4 binary quasar sample to the results from H06. In the left-hand panel, we consider our calculation for all quasars in Table 4, and project the result for both proper and comoving scales by placing all binaries at the mean proper or comoving distance of our sample. In the right-hand panel, we consider binaries in Table 4 with  $23.7 < R_{prop} < 29.7 h^{-1}$  kpc and  $1.0 < z < 2.1$ . We additionally include SDSSJ1635+2911 in this second sample, as we are spatially complete for component separations of  $23.7 < R_{prop} < 29.9$  for  $1.03 < z < 2.1$ .

Figure 4 demonstrates that our results, using a complete, statistical sample of UVX binary quasars are broadly consistent with H06. To compare with H06 we fit power laws, displayed in Figure 4, out to proper (comoving) scales of  $< 100 h^{-1}$  kpc ( $< 200 h^{-1}$  kpc), and integrate them over our scales of interest. At the mean redshift ( $\bar{z} = 1.40$ ) of our sample,  $3.9'' < \theta < 5.2''$ , the range for which our sample is complete, is equivalent to proper (comoving) scales of  $23.5 h^{-1}$  kpc  $< R_{prop} < 31.4 h^{-1}$  kpc ( $56.5 h^{-1}$  kpc  $< R < 75.3 h^{-1}$  kpc). Over this angular range, we find  $\overline{W}_p = 30.8 \pm_{11.0}^{15.7}$  for our data. The proper (comoving) power-law fit to the data from H06, implies  $\overline{W}_p = 55.1$  (60.4) over the same scales, a  $1.5\sigma$  ( $1.9\sigma$ ) difference. The difference is slightly more pronounced if we determine  $\overline{W}_p$  for the H06 data at the mean scale of the 8 binaries in our sample, instead of projecting  $3.9'' < \theta < 5.2''$  back to  $z = 1.4$ . For the 5 binaries in our spatially complete clustering subsample, which covers scales of  $23.7 h^{-1}$  kpc  $< R_{prop} < 29.9 h^{-1}$  kpc, we find  $\overline{W}_p = 24.0 \pm_{10.8}^{16.9}$ , and the H06 data implies  $\overline{W}_p = 57.2$ , 2.4 times (and  $2.0\sigma$ ) higher than our result.

## 5. DISCUSSION

We find that the projected correlation function of quasars at proper scales of  $\sim 25 h^{-1}$  kpc has an amplitude a factor of 2.4 times lower than that determined by H06. H06 argue that clustering on these scales is  $\sim 10$  times higher than expected from projecting

the quasar autocorrelation of Porciani et al. (2004) to smaller scales. Our data thus imply excess quasar clustering at  $\sim 25 h^{-1}$  kpc of a factor of  $\sim 4$ , consistent with the quoted upper limit in M07b. Given that our sample is targeted differently than any previous samples of binary quasars (i.e. UVX but otherwise regardless of the color similarity of the candidate components), and given our simple selection function, our work might be viewed as independently corroborating the evidence for excess quasar clustering on small scales first detected in H06. We note that our binary quasar clustering subsample is largely independent of the sample used by H06, as of the 8 binaries listed in Table 4 only 2 appear in Table 2.

At  $R_{prop} \sim 25 h^{-1}$  kpc we find a significantly smaller clustering amplitude than found by H06. As the binaries in Table 4 are all at  $z < 2$  but H06 include several  $R_{prop} \sim 25 h^{-1}$  kpc binaries with  $z > 2$ , an interesting possibility is that  $\overline{W}_p$  is a function of scale and redshift. Certainly, on large scales ( $\gtrsim 1 h^{-1}$  Mpc), quasars cluster twice as strongly at  $z > 2$  than at  $z < 1$  (e.g., Croom et al. 2005; Shen et al. 2007). The mean redshift of the H06 sample is  $\bar{z} = 1.87$  (J. Hennawi 2007, private communication) compared to  $\bar{z} = 1.42$  for our sample in Table 4. Croom et al. (2005) estimate quasar bias on large (i.e.,  $\gtrsim 1 h^{-1}$  Mpc) scales to follow  $b(z) = 0.53 + 0.289(1+z)^2$ . Given that quasar clustering scales as  $b^2$ , the implied relative amplitude between quasar clustering in H06 and our sample is  $\sim 1.72$ . Scaling our measurement of  $\overline{W}_p = 30.8 \pm_{11.0}^{15.7}$  by this factor implies  $\overline{W}_p = 53.0 \pm_{18.9}^{27.0}$ , easily consistent with the value of  $\overline{W}_p = 57.2$  implied by our fit to H06 in Figure 4. Scaling the  $\overline{W}_p = 24.0 \pm_{10.8}^{16.9}$  estimate for our complete subsample ( $\bar{z} = 1.60$ ) in the same way implies  $\overline{W}_p = 33.1 \pm_{14.9}^{23.4}$ , lower than  $\overline{W}_p = 57.2$  but consistent to  $\sim 1\sigma$ . Thus, multiplying our quasar clustering amplitudes on *small* scales by the implied bias evolution from quasar clustering on *large* scales somewhat reconciles our clustering amplitudes with the higher redshift results from H06. Consistent evolution of quasar clustering on large and small scales is a natural feature of merger-driven models of quasar origin (e.g., Figure 17 of Hopkins et al. 2007b).

We can also look for direct redshift dependence within our sample. Splitting the sample in Table 4 at  $z = 1.55$ , we find  $\overline{W}_p = 27.9 \pm_{13.9}^{22.9}$  for  $z < 1.55$  ( $\bar{z} \sim 1.07$ ) and  $\overline{W}_p = 34.9 \pm_{17.2}^{28.4}$  for  $z > 1.55$  ( $\bar{z} \sim 1.76$ ). Although these results seem consistent, the mean separation of the binaries at  $z < 1.55$  ( $z > 1.55$ ) is  $R_{prop} = 23.8$  (28.4). The power law fits displayed in Figure 4 imply that we should therefore expect quasars to be  $\sim 30\%$  more clustered at  $z < 1.55$  than at  $z > 1.55$ . Incorporating this  $\sim 30\%$  correction, we measure the ratio of the amplitudes of  $\overline{W}_p$  at  $z > 1.55$  and  $z < 1.55$  to be  $1.62 \pm 1.54$ . Although not a very significant detection, a factor of  $1.62 \pm 1.54$  is again consistent with quasar clustering evolution on large scales, as a  $b(z) = 0.53 + 0.289(1+z)^2$  bias relation implies a ratio of  $\sim 2.4$  between the amplitudes of  $\overline{W}_p$  at  $z = 1.76$  and  $z = 1.07$ .

Our analyses could be easily extended, as the 98 ( $3'' \leq \Delta\theta < 6''$ ) DR4 KDE binary quasar candidates should contain  $\sim 40$  binary quasars. Based on our  $\overline{W}_p$

estimates, such a sample is the minimum necessary to detect any redshift dependence to quasar clustering at  $R_{prop} \sim 25 h^{-1}$  kpc, providing only a  $\sim 1.5\sigma$  detection. Completing this sample on a 4-meter class telescope would likely require dark time, as 14 of the DR4 binary candidates have a component at  $g > 21$ . Alternatively, Shen et al. (2007) suggest a survey of quasar pairs at  $z > 3$ , where stronger quasar clustering may lead to a more significant detection of evolution. The DR6 KDE quasar catalog (Richards et al, in prep), which will be selected to  $i < 21$  ( $g \lesssim 21.25$ ), should contain  $\sim 500$  binary quasar candidates across a large redshift range ( $0.4 \lesssim z \lesssim 5$ ) with which to pursue this goal in a single homogeneous sample.

## 6. CONCLUSIONS

We have presented a spectroscopic survey of binary quasar candidates with separations in the range  $3'' \leq \Delta\theta < 6''$ . Our candidates (see Table 1 of M07b) are a subsample of quasars photometrically classified in SDSS DR4 using the KDE technique of Richards et al. (2004). We define a binary as a quasar pair with a line-of-sight velocity difference of  $|\Delta v_{||}| < 2000 \text{ km s}^{-1}$  (see H06). We present 27 new sets of observations and identify both members of 22 candidate binary quasars. Of the 22 new pairs, 10 turn out to be binary quasars (of which  $\sim 2$  might actually be lenses). This roughly doubles the number of known binary quasars with  $3'' \leq \Delta\theta < 6''$  at  $z \lesssim 2$  and  $g < 21$ . A further 9 of our observed candidates are projected quasar pairs, and 3 contain a NELG or star. This confirms that the KDE technique is  $\sim 95\%$  efficient at selecting quasars (e.g., Richards et al. 2004; Myers et al. 2006, 2007a). Combined with observations from the literature (mainly from H06), 46% of the DR4 KDE binary quasar candidates have now been observed, of which  $\sim 47\%$  are binaries or lenses,  $\sim 40\%$  are projected quasar pairs, and the remainder contain a non-quasar.

As our candidate binaries, beyond a UVX cut, are selected regardless of the *relative* colors of the quasars in the pair, we can try to assess the color similarity criteria that optimally select binary quasars. For quasars pre-selected with an already efficient approach such as the KDE technique, we find that a  $\chi^2$  color similarity statistic of  $\chi_{color}^2 < 70$  will return 97% of binaries, lenses and projected pairs (multiplied by the 95% completeness of the KDE technique itself) at 93% efficiency. Most of this efficiency in selecting quasar pairs comes from the KDE technique itself, as imposing no color similarity criterion is 87% efficient. To select binary quasars, while rejecting projected quasar pairs, we recommend a cut in the overlap of the photometric redshifts of the two candidate quasars in a pair. An overlap of  $\gtrsim 0.03$  in the primary solution for the photometric redshift probability functions of the pair can be constructed to be  $\sim 95\%$  complete and  $\sim 70\%$  efficient for binary quasars. Similarly, of course, the reverse probability cut of  $\lesssim 0.03$ , perhaps coupled with a  $\chi_{color}^2 < 70$  cut to remove stars, can be used to reject binary quasars in favor of projected quasar pairs.

We measure the clustering of a complete sample of DR4 binaries on proper scales of  $23.7 < R_{prop} < 29.7 h^{-1}$  kpc. We find that, at  $\sim 25 h^{-1}$  kpc, quasars cluster with an amplitude 2.4 times, or  $2.0\sigma$ , lower than determined by

H06. As the mean redshift of the H06 sample is  $\bar{z} = 1.87$  compared to  $\bar{z} = 1.40$  for our sample, this can be interpreted as evidence of evolution in quasar clustering on scales of  $\sim 25 h^{-1}$  kpc. The implied evolution is broadly consistent with merger-driven models, where the quasar population is expected to evolve with consistent large-to-small scale clustering (e.g., Hopkins et al. 2007b). We find no significant evidence for quasar clustering evolution at  $\sim 25 h^{-1}$  kpc, from  $\bar{z} \sim 1.07$  to  $\bar{z} \sim 1.76$ , in our sample alone. Assuming evolution in the binary quasar population at the level suggested by our current sample, we argue that the 98 quasars in the DR4 KDE candidate binary sample will detect any clustering evolution at proper scales of  $\sim 25 h^{-1}$  kpc at  $\sim 1.5\sigma$  significance. A sample of  $\sim 200$  candidates ( $\sim 80$  binary quasars) will be necessary to definitively detect clustering evolution at  $\sim 25 h^{-1}$  kpc for  $z \lesssim 2.5$ .

We thank the NOAO staff for their indispensable help and knowledge. In particular, we thank Buell Januzzi, without whose support this work would not have been possible in a timely fashion. ADM and RJB acknowledge support from NASA through grant NN6066H156, from Microsoft Research, and from the University of Illinois. DPS acknowledges NSF support through grant AST-0607634. PBH is supported by NSERC. The authors made extensive use of the storage and computing facilities at the National Center for Supercomputing Applications and thank the technical staff for their assis-

tance in enabling this work. We thank Robert Nichol and Alex Gray for their invaluable work on the KDE catalog.

Funding for the SDSS and SDSS-II has been provided by the Alfred P. Sloan Foundation, the Participating Institutions, the National Science Foundation, the U.S. Department of Energy, the National Aeronautics and Space Administration, the Japanese Monbukagakusho, the Max Planck Society, and the Higher Education Funding Council for England. The SDSS Web Site is <http://www.sdss.org/>.

The SDSS is managed by the Astrophysical Research Consortium for the Participating Institutions. The Participating Institutions are the American Museum of Natural History, Astrophysical Institute Potsdam, University of Basel, Cambridge University, Case Western Reserve University, University of Chicago, Drexel University, Fermilab, the Institute for Advanced Study, the Japan Participation Group, Johns Hopkins University, the Joint Institute for Nuclear Astrophysics, the Kavli Institute for Particle Astrophysics and Cosmology, the Korean Scientist Group, the Chinese Academy of Sciences (LAMOST), Los Alamos National Laboratory, the Max-Planck-Institute for Astronomy (MPIA), the Max-Planck-Institute for Astrophysics (MPA), New Mexico State University, Ohio State University, University of Pittsburgh, University of Portsmouth, Princeton University, the United States Naval Observatory, and the University of Washington.

#### REFERENCES

- Adelman-McCarthy, J. K., et al. 2006, *ApJS*, 162, 38  
Antonucci, R. 1993, *ARA&A*, 31, 473  
Bahcall, J. N., Bahcall, N. A., & Schneider, D. P. 1986, *Nature*, 323, 515  
Bahcall, J. N., Kirhakos, S., Saxe, D. H., & Schneider, D. P. 1997, *ApJ*, 479, 642  
Barnes, J. E., & Hernquist, L. 1996, *ApJ*, 471, 115  
Cao, L., Wei, J.-Y., & Hu, J.-Y. 1999, *A&AS*, 135, 243  
Croom, S. M., & Shanks, T. 1996, *MNRAS*, 281, 893  
Croom, S. M., et al. 2005, *MNRAS*, 356, 415  
Djorgovski, S. 1991, in *ASP Conf. Ser. 21, The Space Distribution of Quasars*, ed. D. Crampton (San Francisco: ASP), 349  
Djorgovski, S., & Spinrad, H. 1984, *ApJ*, 282, L1  
Djorgovski, S. G., Courbin, F., Meylan, G., Sluse, D., Thompson, D., Mahabal, A., & Glikman, E. 2007, *ApJ*, 662, L1  
Elvis, M. 2000, *ApJ*, 545, 63  
Fukugita, M., Ichikawa, T., Gunn, J. E., Doi, M., Shimasaku, K., & Schneider, D. P. 1996, *AJ*, 111, 1748  
Gehrels, N. 1986, *ApJ*, 303, 336  
Hennawi, J. F., et al. 2006, *AJ*, 131, 1 (H06)  
Hewett, P. C., Foltz, C. B., Chaffee, F. H., Francis, P. J., Weymann, R. J., Morris, S. L., Anderson, S. F., & MacAlpine, G. M. 1991, *AJ*, 101, 1121  
Hewett, P. C., Foltz, C. B., Harding, M. E., & Lewis, G. F. 1998, *AJ*, 115, 383  
Hopkins, P. F., & Hernquist, L. 2006, *ApJS*, 166, 1  
Hopkins, P. F., Hernquist, L., Cox, T. J., Di Matteo, T., Robertson, B., & Springel V. 2006, *ApJS*, 163, 1  
Hopkins, P. F., Lidz, A., Hernquist, L., Coil, A. L., Myers, A. D., Cox, T. J., & Spergel, D. N. 2007, *ApJ*, 662, 110  
Hopkins, P. F., Hernquist, L., Cox, T. J., & Keres, D. 2007, *ArXiv e-prints*, 706, [arXiv:0706.1243](http://arxiv.org/abs/0706.1243)  
Inada, N., et al. 2003, *Nature*, 426, 810  
Kochanek, C. S., Falco, E. E., & Muñoz, J. A. 1999, *ApJ*, 510, 590  
Landy, S. D., & Szalay, A. S. 1993, *ApJ*, 412, 64  
Lupton, R., Gunn, J. E., & Szalay, A. S. 1999, *AJ*, 118, 1406  
Mason, K. O., et al. 2000, *MNRAS*, 311, 456  
Mortlock, D. J., Webster, R. L., & Francis, P. J. 1999 *MNRAS*, 309, 836  
Myers, A. D., et al. 2006, *ApJ*, 638, 622  
Myers, A. D., et al. 2007a, *ApJ*, 658, 85  
Myers, A. D., et al. 2007b, *ApJ*, 658, 99 (M07b)  
Oguri, M. 2006, *MNRAS*, 367, 1241  
Oguri, M., et al. 2005, *ApJ*, 622, 106  
Inada, N., et al. 2007, *ArXiv e-prints*, 708, [arXiv:0708.0828](http://arxiv.org/abs/0708.0828)  
Peng, C. Y., et al. 1999, *ApJ*, 524, 572  
Phinney, E. S., & Blandford, R. D. 1986, *Nature*, 321, 569  
Pogson, N. R. 1856, *MNRAS*, 17, 12  
Porciani, C., Magliocchetti, M., & Norberg, P. 2004, *MNRAS*, 355, 1010  
Richards, G. T., et al. 2001, *AJ*, 121, 2308  
Richards, G. T., et al. 2004, *ApJS*, 155, 257  
Rusin, D., 2002, *ApJ*, 572, 705  
Schlegel, D. J., Finkbeiner, D. P., & Davis, M. 1998, *ApJ*, 500, 525  
Schneider, D. P., et al. 2003, *AJ*, 126, 2579  
Schneider, D. P., et al. 2007, *AJ*, 134, 102  
Shanks, T., Bean, A. J., Ellis, R. S., Fong, R., Efstathiou, G., & Peterson, B. A. 1983, *ApJ*, 274, 529  
Shen, Y., et al. 2007, *AJ*, 133, 2222  
Spergel, D. N., et al. 2007, *ApJS*, 170, 377  
Sramek, R. A., & Weedman, D. W. 1978, *ApJ*, 221, 468  
Stoughton, C., et al. 2002, *AJ*, 123, 485  
Tonry, J., & Davis, M. 1979, *AJ*, 84, 1511  
Weinstein, M. A., et al. 2004, *ApJS*, 155, 243  
Vanden Berk, D. E., et al. 2001, *AJ*, 122, 549  
Veron-Cetty, M.-P., et al. 2004, *A&A*, 414, 487  
York, D. G., et al. 2000, *AJ*, 120, 1579

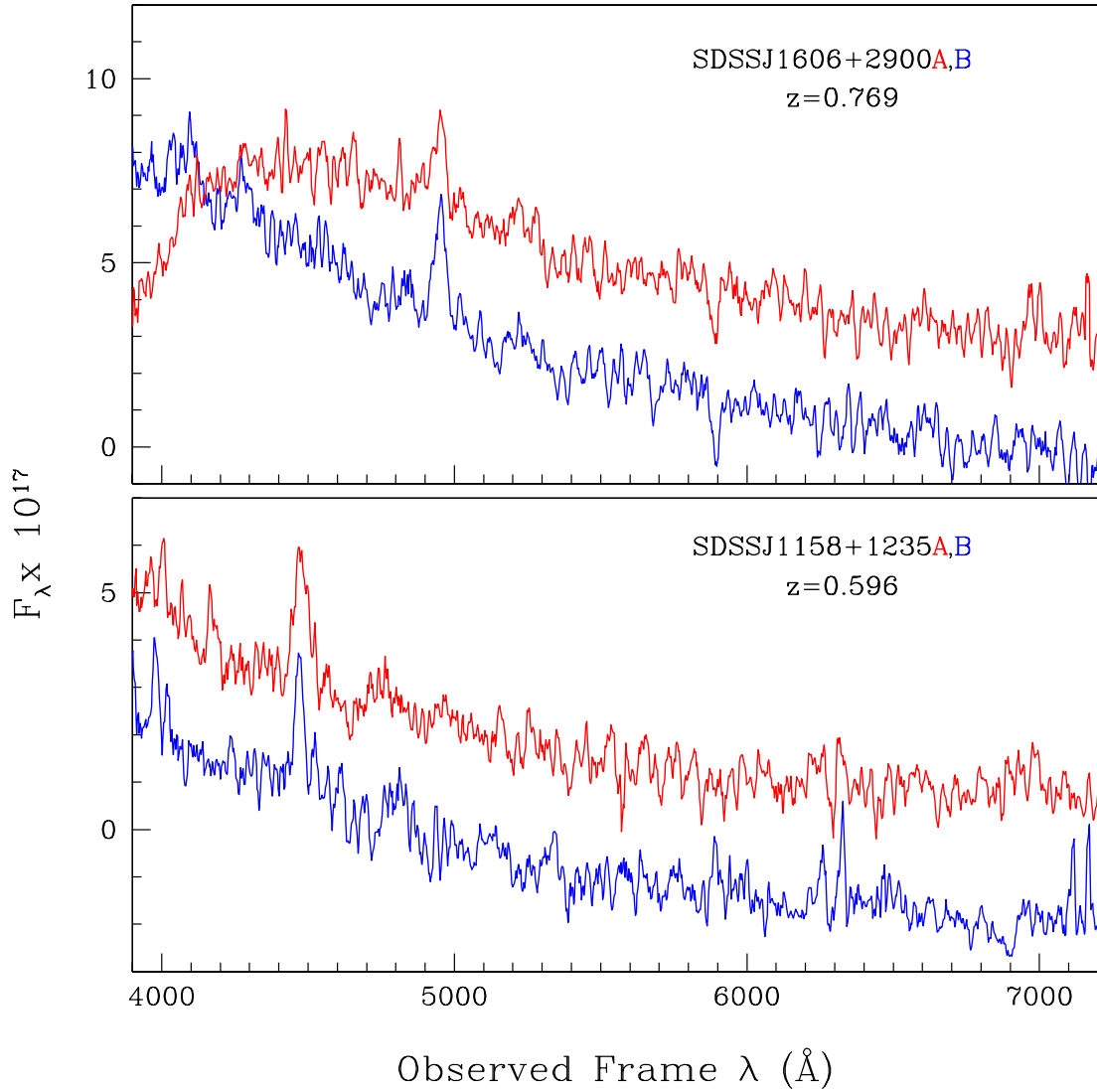


FIG. 1.— Two of the five quasar pairs in our DR4 KDE sample that require higher resolution spectroscopy to determine whether they are binary quasars or a lensed quasar. These spectra were taken with the R-C Spectrograph on the Mayall 4-m at KPNO at a resolution  $\sim 5\text{\AA}$ , and have been smoothed with a 5 pixel boxcar. SDSSJ1158+1235A,B and SDSSJ1606+2900A,B are our two most likely lens candidates, based on their similar colors and component separations of  $\Delta\theta < 4''$ . In both panels, component A is the upper spectrum and component B has been offset, which can cause component B to have a flux density below zero. In each case, both components are, in reality, at nearly identical flux levels.

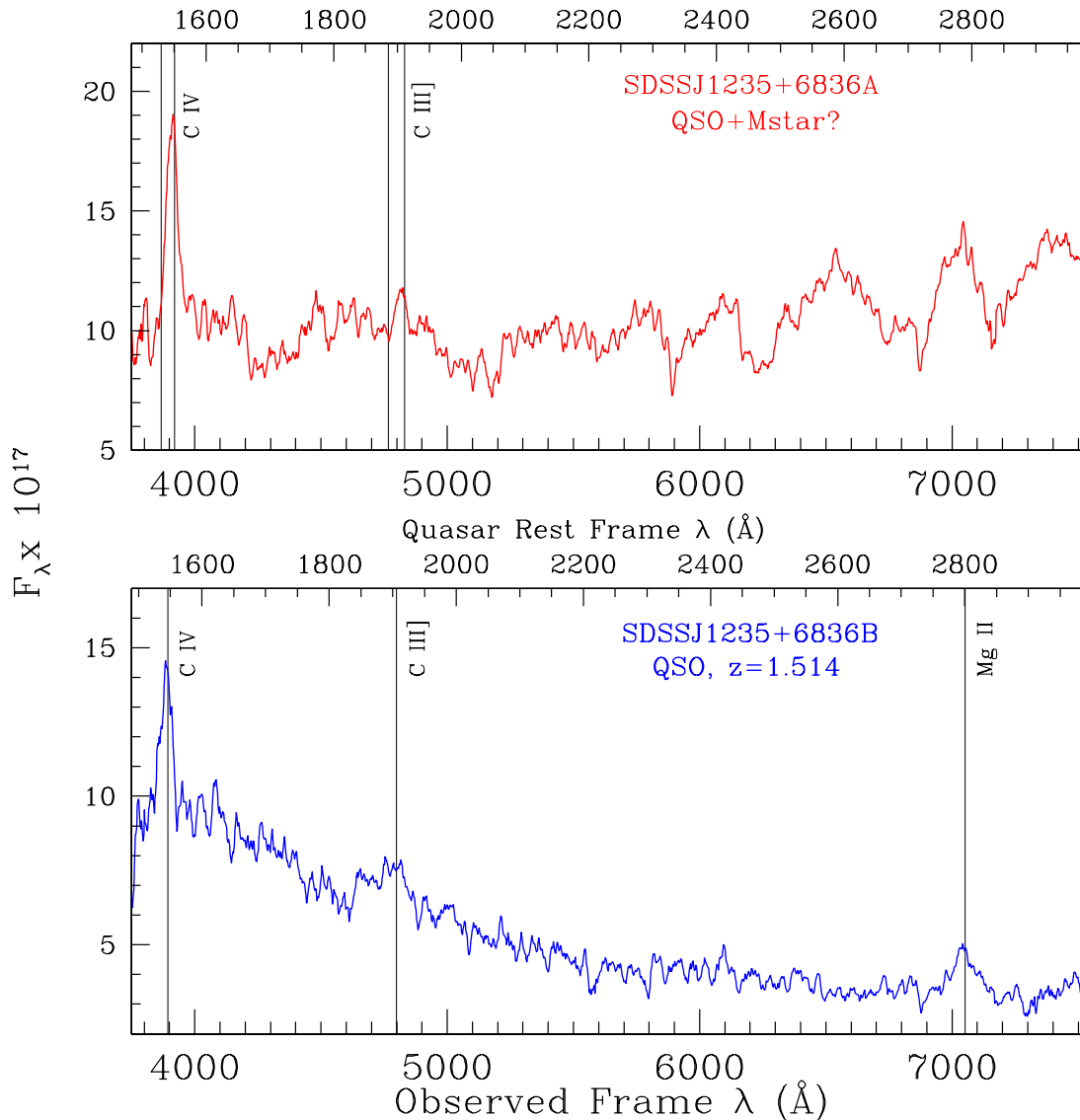


FIG. 2.— Spectra of SDSSJ1235+6836A,B taken with the R-C Spectrograph on the Mayall 4-m at KPNO at a resolution  $\sim 5\text{\AA}$ , and smoothed with a 5 pixel boxcar. In the lower panel, the vertical lines mark common quasar emission lines. For component A, in the upper panel, emission lines are marked at the systemic redshift of *component B* offset by  $\pm 2000 \text{ km s}^{-1}$ , a typical window for a binary quasar (e.g., H06). The systemic redshift of component A in Table 1d is derived assuming the emission line near  $3900\text{\AA}$  is CIV, and is close to the red side of these windows ( $z = 1.529$ ). At red wavelengths, component A resembles an M star.

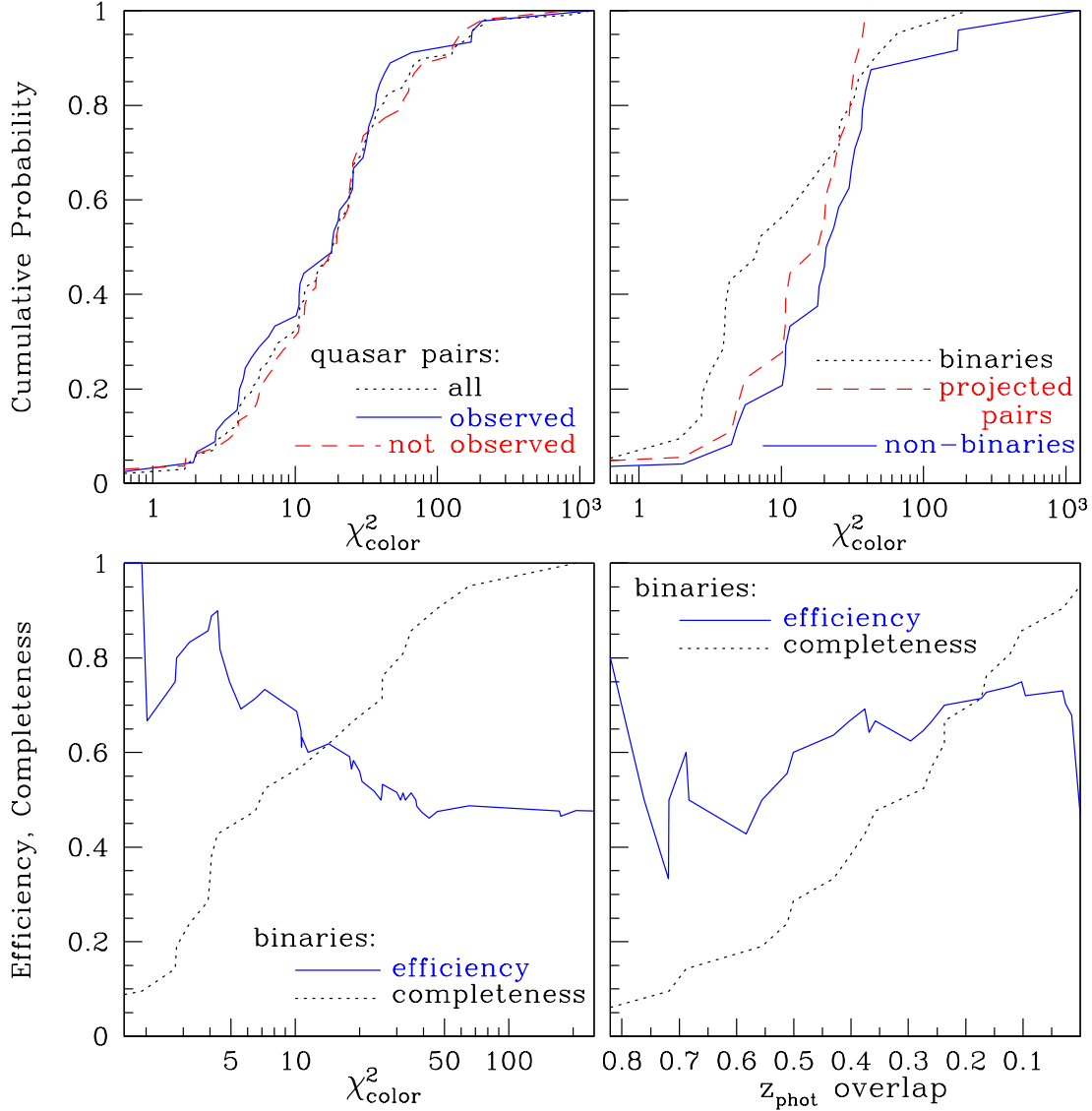


FIG. 3.— *Upper-left:* The cumulative probability distribution of the  $\chi^2_{color}$  color similarity statistic (Equation 1) for the 45 spectroscopically observed DR4 KDE candidate binary quasars, the 53 that are not yet observed, and for all 98 candidate pairs. *Upper-right:* Similar to upper-left, but for the 21/45 observed candidates that are binary quasars (or lenses), for the 24/45 that are not binaries and for the 18/45 quasar pairs at disjoint redshifts. *Lower-left:* The selection completeness and efficiency effects of imposing a  $\chi^2_{color}$  limit on the 45 observed DR4 KDE candidate binaries. Efficiency is (number of binaries  $< \chi^2_{color}$ )/(total candidates  $< \chi^2_{color}$ ); completeness is (number of binaries or lenses  $< \chi^2_{color}$ )/21. *Lower-right:* Similar to lower-left, but using the fractional overlap of the photometric redshift solutions for the candidate components ( $z_{phot}$ ) as the determinant of binary selection. Note that more overlap in photometric redshift implies greater color similarity.

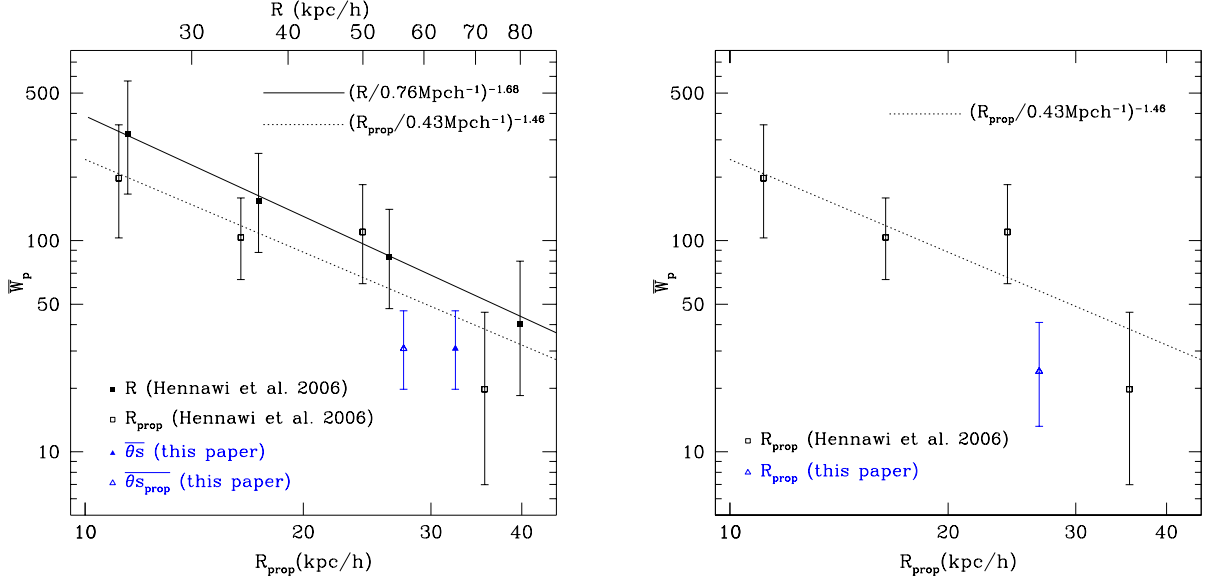


FIG. 4.— The projected correlation function,  $\overline{W}_p$ , of quasars on small scales. *Left*: The results of H06 in proper (lower axis) and comoving (upper axis) coordinates are compared to our mean DR4 KDE spectroscopic results averaged over  $3.9'' < \Delta\theta < 5.2''$  and projected to a mean transverse separation at  $z = 1.4$  (the mean redshift of both the DR4 KDE quasar sample and the subset of 16 quasars listed in Table 4), in proper (open triangle) and comoving (solid triangle) coordinates. The dashed (solid) line shows a power law fit to the H06 data on proper (comoving) scales  $< 100 h^{-1} \text{ kpc}$  ( $< 200 h^{-1} \text{ kpc}$ ). *Right*: A similar comparison but our data are now averaged over scales of  $23.7 < R_{prop} < 29.7 h^{-1} \text{ kpc}$  and redshifts of  $1.0 < z < 2.1$ . The DR4 KDE binary quasar sample is spectroscopically complete for  $A_g < 0.17$ ,  $g < 20.85$ , and  $3.9'' < \Delta\theta < 5.2''$ , and for  $23.7 < R_{prop} < 29.7 h^{-1} \text{ kpc}$  over  $1.0 < z < 2.1$ .

TABLE 1A  
DR4 KDE CANDIDATE BINARIES FOR WHICH WE HAVE OBSERVED ONE MEMBER

$\Delta\theta$	$\chi_{color}^2$	Name	$\alpha$ (J2000)	$\delta$ (J2000)	$g$	$z_{phot}$ range	SDSS $z$	Our $z$
5.50	36.2	SDSSJ093014.81+420038.7	09 30 14.816	+42 00 38.71	19.71	1.15,1.425,1.50,0.93		0.544 <sup>?</sup>
		SDSSJ093015.01+420033.6	09 30 15.016	+42 00 33.68	20.03	1.85,2.025,2.15,0.62		
5.55	24.2	SDSSJ093521.02+641219.8	09 35 21.020	+64 12 19.89	20.99	1.45,1.775,2.10,0.92		1.566
		SDSSJ093521.80+641221.9	09 35 21.807	+64 12 22.00	20.96	0.25,0.375,0.45,0.66		
5.33	6.4	SDSSJ095840.74+332216.3	09 58 40.746	+33 22 16.31	19.18	1.35,1.475,2.10,0.84	1.891	1.888
		SDSSJ095840.94+332211.5	09 58 40.945	+33 22 11.59	20.64	1.45,1.725,2.10,0.91		
3.46	161	SDSSJ103939.31+100253.0	10 39 39.317	+10 02 53.01	18.42	0.10,0.175,0.25,0.56	0.161	0.161
		SDSSJ103939.53+100254.3	10 39 39.532	+10 02 54.40	19.60	0.65,1.125,1.55,0.92		
4.22	8.2	SDSSJ162847.75+413045.4	16 28 47.752	+41 30 45.45	19.81	1.35,1.525,1.70,0.85		
		SDSSJ162848.06+413043.1	16 28 48.069	+41 30 43.19	20.40	1.95,2.075,2.20,0.63		0.831 <sup>?</sup>

NOTE. — The angular pair separations are denoted  $\Delta\theta$  (″), and  $\chi_{color}^2$  is each pair’s color similarity statistic (Equation 1). The photometric redshifts  $z_{phot}$  are expressed as “lowest extent, peak, highest extent, probability of true redshift lying in this range”. The “SDSS  $z$ ” column shows matches to any spectroscopic object in the SDSS DR6 Catalog Archive Server (mainly, e.g., Schneider et al. 2007). The “Our  $z$ ” column lists our new spectroscopic confirmations from KPNO data. In the “SDSS  $z$ ” and “Our  $z$ ” columns the object is a quasar at the provided redshift, unless otherwise noted. Redshifts labeled with a ? are based on a single emission line, which is reasonably assumed to be Mg II.  $g$  is not corrected for Galactic extinction.

TABLE 1B  
CONFIRMED BINARY QUASARS IN THE DR4 KDE CANDIDATE SAMPLE

$\Delta\theta$	$\chi_{color}^2$	Name	$\alpha$ (J2000)	$\delta$ (J2000)	$g$	$z_{phot}$ range	SDSS $z$	Our $z$
*3.56	4.0	SDSSJ1158+1235A	11 58 22.776	+12 35 18.59	19.90	0.45,0.525,0.65,0.55		0.596 <sup>?</sup>
		SDSSJ1158+1235B	11 58 22.989	+12 35 20.31	20.12	0.40,0.475,0.65,0.63		0.596 <sup>?</sup>
*4.74	32.0	SDSSJ1320+3056A	13 20 22.545	+30 56 22.87	18.60	1.35,1.475,1.65,0.90	1.597	1.595
		SDSSJ1320+3056B	13 20 22.643	+30 56 18.29	19.92	1.45,1.575,1.80,0.51		1.596
*4.50	2.8	SDSSJ1418+2441A	14 18 55.418	+24 41 08.92	19.27	0.45,0.525,0.70,0.96	0.573	0.572
		SDSSJ1418+2441B	14 18 55.536	+24 41 04.71	20.22	0.40,0.625,0.70,0.86		0.573
4.27	3.2	SDSSJ1426+0719A	14 26 04.266	+07 19 25.86	20.82	0.95,1.175,1.45,0.99		1.312
		SDSSJ1426+0719B	14 26 04.326	+07 19 30.04	20.12	1.00,1.225,1.45,0.97		1.309
5.41	25.6	SDSSJ1430+0714A	14 30 02.664	+07 14 15.62	20.27	1.00,1.225,1.40,0.97		1.246
		SDSSJ1430+0714B	14 30 02.886	+07 14 11.33	19.50	1.05,1.375,1.45,0.97	1.258	1.261
5.14	65.6	SDSSJ1458+5448A	14 58 26.165	+54 48 14.85	20.79	1.50,1.775,1.95,0.75		1.913
		SDSSJ1458+5448B	14 58 26.728	+54 48 13.19	20.53	1.65,1.925,1.95,0.47		1.912
*3.45	10.8	SDSSJ1606+2900A	16 06 02.812	+29 00 48.79	18.50	0.50,0.725,1.00,0.65	0.770	0.769 <sup>?</sup>
		SDSSJ1606+2900B	16 06 03.021	+29 00 50.88	18.42	0.70,0.875,1.00,0.92		0.769 <sup>?</sup>
*4.92	25.6	SDSSJ1635+2911A	16 35 10.148	+29 11 20.65	18.83	1.45,1.575,1.80,0.84	1.586	1.582
		SDSSJ1635+2911B	16 35 10.306	+29 11 16.19	20.43	1.40,1.525,1.85,0.79		1.590

NOTE. — We define a binary quasar by a line-of-sight velocity difference of  $|\Delta v_{||}| < 2000$  km s<sup>-1</sup> in the rest-frame of either component. The pair containing SDSSJ143002.66+071415.6 has velocity difference  $|\Delta v_{||}| = 2000 \pm 400$  km s<sup>-1</sup>, just inside our definition of a binary. Components are denoted A and B so that the position angle from A to B lies between 0° and 180°. A preceding \* denotes that our spectroscopy alone is insufficient to rule out a lens interpretation for this pair (see §2.2.1). SDSSJ1320+3056A first appeared with a confirmed redshift ( $z=1.587$ ) in Veron-Cetty et al. (2004).  $g$  is not corrected for Galactic extinction. See Table 1a for additional notes describing shared notation.

TABLE 1c  
 CONFIRMED PROJECTED PAIRS IN THE DR4 KDE CANDIDATE SAMPLE

$\Delta\theta$	$\chi^2_{color}$	Name	$\alpha$ (J2000)	$\delta$ (J2000)	$g$	$z_{phot}$ range	SDSS $z$	Our $z$
4.28	1220	SDSSJ083258.34+323003.3 SDSSJ083258.56+323000.0	08 32 58.348 08 32 58.567	+32 30 03.35 +32 30 00.08	19.96 19.59	2.75,2.775,2.80,0.88 0.40,0.425,0.50,0.70		0.397 star
3.42	2.0	SDSSJ084257.37+473342.5 SDSSJ084257.63+473344.7	08 42 57.378 08 42 57.638	+47 33 42.56 +47 33 44.74	19.00 20.45	0.50,0.625,0.70,0.51 0.85,1.775,2.10,0.84	1.552	1.554 1.681
4.28	4.9	SDSSJ085914.77+424123.6 SDSSJ085915.15+424123.5	08 59 14.771 08 59 15.159	+42 41 23.67 +42 41 23.58	21.02 19.22	0.95,1.375,1.65,0.66 0.80,0.975,1.40,0.93	0.898	1.396 0.902 <sup>?</sup>
4.57	20.6	SDSSJ094309.36+103401.3 SDSSJ094309.66+103400.6	09 43 09.363 09 43 09.670	+10 34 01.31 +10 34 00.65	20.07 19.24	0.95,1.525,1.70,0.80 1.05,1.325,1.40,0.99	1.238	1.431 1.240
5.91	32.8	SDSSJ111053.63+605347.9 SDSSJ111054.10+605343.1	11 10 53.633 11 10 54.105	+60 53 47.97 +60 53 43.16	18.94 20.86	0.65,0.775,0.90,0.96 1.55,1.775,2.20,0.68		0.793 0.552 <sup>?</sup>
5.19	18.4	SDSSJ112556.32+143148.0 SDSSJ112556.54+143152.1	11 25 56.321 11 25 56.549	+14 31 48.10 +14 31 52.10	20.70 20.38	0.90,1.325,1.60,0.69 1.50,1.725,2.15,0.97		NELG 1.924
5.78	29.9	SDSSJ113637.52+563500.4 SDSSJ113638.09+563503.9	11 36 37.526 11 36 38.090	+56 35 00.48 +56 35 03.90	19.94 19.02	1.85,2.075,2.15,0.63 0.60,0.675,0.90,0.56		1.282 2.672
4.92	39.3	SDSSJ114503.06+660211.3 SDSSJ114503.74+660208.6	11 45 03.063 11 45 03.741	+66 02 11.35 +66 02 08.67	20.09 20.24	1.65,1.825,2.00,0.89 0.50,0.675,0.85,0.52		1.732 2.304
3.26	11.5	SDSSJ123122.27+493433.8 SDSSJ123122.37+493430.7	12 31 22.276 12 31 22.378	+49 34 33.86 +49 34 30.75	20.63 19.94	0.50,0.725,0.90,0.53 1.55,1.775,2.15,0.95		0.780 <sup>?</sup> 1.811 <sup>?</sup>
4.00	10.7	SDSSJ150656.86+505610.5 SDSSJ150657.18+505607.9	15 06 56.866 15 06 57.183	+50 56 10.56 +50 56 07.92	19.22 19.75	0.65,0.775,1.00,0.75 2.00,2.225,2.40,0.45		0.775 <sup>?</sup> 2.204

NOTE. — SDSSJ112556.32+143148.0, the NELG, has redshift  $z=0.246$ . Subsequent to our observations, SDSSJ094309.36+103401.3 appeared in Inada et al. (2007), with  $z = 1.433$ .  $g$  is not corrected for Galactic extinction. The redshift for SDSSJ123122.37+493430.7 is based on a single CIV emission line, with weak confirming C III]. See Table 1a for additional notes describing shared notation.

TABLE 1d  
 AMBIGUOUS PAIRS IN THE DR4 KDE BINARY QUASAR CANDIDATE SAMPLE

$\Delta\theta$	$\chi^2_{color}$	Name	$\alpha$ (J2000)	$\delta$ (J2000)	$g$	$z_{phot}$ range	SDSS $z$	Our $z$
4.80	42.5	SDSSJ093424.11+421135.0 SDSSJ093424.32+421130.8	09 34 24.112 09 34 24.324	+42 11 35.05 +42 11 30.87	21.01 20.30	1.45,1.675,2.20,0.90 1.00,1.125,1.40,0.99		f/less 1.339
3.95	10.7	SDSSJ120727.09+140817.1 SDSSJ120727.25+140820.3	12 07 27.100 12 07 27.259	+14 08 17.18 +14 08 20.38	20.39 20.27	1.60,1.775,2.00,0.89 1.55,1.775,1.95,0.86		1.801 <sup>?</sup> 1.8 <sup>??</sup>
3.51	207	SDSSJ1235+6836A SDSSJ1235+6836B	12 35 54.783 12 35 55.270	+68 36 24.78 +68 36 27.07	19.04 19.70	2.75,2.775,2.80,0.55 0.50,0.625,1.10,0.51		1.529 <sup>??</sup> 1.514
4.35	14.4	SDSSJ1507+2903A SDSSJ1507+2903B	15 07 46.909 15 07 47.234	+29 03 34.15 +29 03 33.28	20.44 19.97	0.80,0.975,1.25,0.77 0.70,0.775,0.95,0.66		0.875 <sup>?</sup> 0.862 <sup>?</sup>

NOTE. — Redshifts marked ?? are derived from a single emission line. This differs from the ? notation as the redshift is based on similar emission in the other component (rather than simply assuming that the emission is Mg II). The ambiguities, and why we conclude that SDSSJ1235+6836 and SDSSJ1507+2903 are binaries but the other pairs are not, are discussed in §2.2.2.  $g$  is not corrected for Galactic extinction. See Table 1a for additional notes describing shared notation.

TABLE 2  
PREVIOUSLY IDENTIFIED DR4 KDE BINARY QUASAR CANDIDATES ( $3'' \leq \Delta\theta < 6''$ )

$\Delta\theta$	$\chi^2_{color}$	Name	$\alpha$ (J2000)	$\delta$ (J2000)	$g$	$z_{phot}$ range	$z$
<u>Projected pairs</u>							
4.90	36.7	SDSSJ024907.77+003917.1	02 49 07.778	+00 39 17.12	19.36	2.00,2.175,2.25,0.48	2.164
		SDSSJ024907.86+003912.4	02 49 07.866	+00 39 12.40	20.63	0.45,0.675,0.85,0.84	star
4.09	18.0	SDSSJ083649.45+484150.0	08 36 49.456	+48 41 50.08	19.31	0.45,0.675,0.80,0.67	0.657
		SDSSJ083649.55+484154.0	08 36 49.554	+48 41 54.06	18.50	1.50,1.675,1.95,0.94	1.712
5.42	4.5	SDSSJ090235.35+563751.8	09 02 35.356	+56 37 51.84	20.95	1.15,1.275,1.45,0.98	1.39
		SDSSJ090235.73+563756.2	09 02 35.731	+56 37 56.29	20.56	1.05,1.225,1.45,0.98	1.34
3.14	37.1	SDSSJ095454.73+373419.7	09 54 54.735	+37 34 19.79	19.57	0.95,1.475,1.65,0.90	1.544
		SDSSJ095454.99+373419.9	09 54 54.999	+37 34 19.99	18.91	1.45,1.575,1.95,0.94	1.892
4.76	10.2	SDSSJ114718.44+123439.8	11 47 18.448	+12 34 39.84	20.91	1.45,1.625,2.00,0.66	1.583
		SDSSJ114718.66+123436.3	11 47 18.668	+12 34 36.33	19.80	2.15,2.225,2.60,0.54	2.232
3.06	5.6	SDSSJ120450.54+442835.8	12 04 50.543	+44 28 35.89	19.04	0.95,1.125,1.45,0.98	1.144
		SDSSJ120450.78+442834.2	12 04 50.784	+44 28 34.25	19.48	1.35,1.725,1.95,0.78	1.814
5.04	23.3	SDSSJ124948.12+060709.0	12 49 48.127	+06 07 09.04	20.41	2.20,2.325,2.65,0.89	2.001
		SDSSJ124948.17+060714.0	12 49 48.179	+06 07 14.02	20.38	1.85,2.075,2.20,0.58	2.376
3.01	20.0	SDSSJ125530.44+630900.5	12 55 30.445	+63 09 00.51	20.30	1.50,1.675,1.90,0.88	1.753
		SDSSJ125530.82+630902.0	12 55 30.823	+63 09 02.09	20.60	1.10,1.375,1.50,0.98	1.393
4.94	31.2	SDSSJ142359.48+545250.8	14 23 59.484	+54 52 50.83	18.63	1.00,1.175,1.45,0.973	1.409 <sup>I</sup>
		SDSSJ142400.00+545248.7	14 24 00.006	+54 52 48.79	19.93	1.45,1.575,1.90,0.772	0.610 <sup>I</sup>
4.35	25.2	SDSSJ162902.59+372430.8	16 29 02.594	+37 24 30.85	19.17	0.80,0.975,1.10,0.93	0.923
		SDSSJ162902.63+372435.1	16 29 02.634	+37 24 35.17	19.35	0.70,0.925,1.10,0.98	0.906
5.83	176	SDSSJ171334.41+553050.3	17 13 34.414	+55 30 50.36	18.88	1.00,1.375,1.45,0.968	1.276 <sup>I</sup>
		SDSSJ171335.03+553047.9	17 13 35.037	+55 30 47.91	19.11	2.00,2.175,2.20,0.686	star <sup>I</sup>
5.06	172	SDSSJ211157.24+091559.3	21 11 57.248	+09 15 59.33	20.73	0.95,1.275,1.40,0.995	
		SDSSJ211157.26+091554.2	21 11 57.269	+09 15 54.28	19.83	1.00,1.325,1.35,0.983	star <sup>S</sup>
<u>Binary quasars</u>							
3.94	18.8	SDSSJ0959+5449A	09 59 07.060	+54 49 08.09	20.60	1.90,2.025,2.15,0.59	1.956
		SDSSJ0959+5449B	09 59 07.471	+54 49 06.38	20.07	1.40,1.575,2.10,0.90	1.954
3.55	6.5	SDSSJ1259+1241A	12 59 55.464	+12 41 51.06	19.99	1.95,2.175,2.30,0.43	2.180
		SDSSJ1259+1241B	12 59 55.617	+12 41 53.81	20.09	1.90,2.175,2.25,0.52	2.189
3.81	4.3	SDSSJ1303+5100A	13 03 26.144	+51 00 51.00	20.54	1.50,2.075,2.20,0.82	1.686
		SDSSJ1303+5100B	13 03 26.177	+51 00 47.21	20.37	1.60,1.775,2.00,0.93	1.684
3.12	0.5	SDSSJ1337+6012A	13 37 13.085	+60 12 09.70	20.04	1.30,1.775,2.05,0.66	1.721
		SDSSJ1337+6012B	13 37 13.133	+60 12 06.60	18.59	1.50,1.625,1.95,0.94	1.727
5.13	4.1	SDSSJ1432-0106A	14 32 28.949	-01 06 13.55	21.10	1.55,2.125,2.25,0.69	2.082
		SDSSJ1432-0106B	14 32 29.247	-01 06 16.06	17.83	1.90,2.025,2.15,0.96	2.082
4.11	7.2	SDSSJ1530+5304A	15 30 38.564	+53 04 04.03	20.56	1.45,1.575,1.95,0.65	1.531
		SDSSJ1530+5304B	15 30 38.824	+53 04 00.65	20.70	1.40,1.725,2.15,0.93	1.533
3.90	2.8	SDSSJ1637+2636A	16 37 00.881	+26 36 13.71	20.61	0.45,0.575,0.85,0.46	1.961 <sup>D</sup>
		SDSSJ1637+2636B	16 37 00.932	+26 36 09.87	19.36	1.40,1.525,1.80,0.64	1.961 <sup>D</sup>
3.72	3.9	SDSSJ1723+5904A	17 23 17.307	+59 04 42.79	20.31	1.45,1.725,2.25,0.63	1.597
		SDSSJ1723+5904B	17 23 17.421	+59 04 46.41	18.88	1.55,1.725,1.90,0.94	1.604
5.81	35.0	SDSSJ2214+1326A	22 14 26.792	+13 26 52.38	20.64	1.55,2.025,2.20,0.85	1.995
		SDSSJ2214+1326B	22 14 27.032	+13 26 57.01	20.34	1.65,1.825,2.05,0.96	2.002
<u>Confirmed lenses</u>							
3.76	1.9	SDSSJ1004+4112A	10 04 34.800	+41 12 39.29	18.64	1.55,1.725,2.00,0.94	1.734 <sup>i</sup>
		SDSSJ1004+4112B	10 04 34.917	+41 12 42.81	19.04	1.55,1.725,2.15,0.79	1.734 <sup>i</sup>
3.04	46.4	SDSSJ1206+4332A	12 06 29.648	+43 32 17.57	18.78	1.65,1.825,2.05,0.96	1.789 <sup>o</sup>
		SDSSJ1206+4332B	12 06 29.652	+43 32 20.61	19.38	1.95,2.175,2.35,0.53	1.789 <sup>o</sup>

NOTE. — Components of a binary are denoted A and B so that the position angle from A to B lies between  $0^\circ$  and  $180^\circ$ . This convention differs from H06, from which we take identifications and redshifts, except for objects labeled *S* (taken from the SDSS), *D* (discovered by Sramek & Weedman 1978, confirmed as a possible lens by Djorgovski & Spinrad 1984, and likely a binary instead, e.g., Kochanek et al. 1999; Peng et al. 1999; Rusin 2002), *i* (part of the quad lens from Inada et al. 2003), *o* (Oguri et al. 2005), and *I* (Inada et al. 2007). Both quasars SDSSJ162902.59+372430.8 and SDSSJ162902.63+372435.1 first appear in Mason et al. (2000). SDSSJ1004+4112A was discovered by Cao et al. (1999), and SDSSJ1432-0106B by Hewett et al. (1991). We note that we mistakenly listed SDSSJ095454.73+373419.7 as lying at  $z=1.554$  in M07b.  $g$  is not corrected for Galactic extinction. See Table 1a for additional notes describing shared notation.

TABLE 3  
BREAKDOWN OF ( $3'' \leq \Delta\theta < 6''$ ) DR4 KDE QUASAR PAIRS

Category	Number of Confirmed Pairs
Total binary quasar candidates	98
Total now identified	45
Likely binary quasars	19
Quasar pairs separated in redshift	18
Pairs containing $\geq 1$ non-quasars	6
Pairs that are confirmed lenses	2

NOTE. — It is possible that a few more objects listed as “Likely binary quasars” may turn out to be a lensed quasar when scrutinized at higher resolution.

TABLE 4  
COMPLETE, STATISTICAL, CLUSTERING SUBSAMPLE

Name	$\Delta\theta''$	$\chi^2_{color}$	$R_{prop}$	$R$	$z_A$	$z_B$	$ \Delta v_{\parallel} $	Table
SDSSJ0959+5449	3.94	18.8	23.8	70.2	1.956	1.954	200	(2)
SDSSJ1320+3056	*4.74	32.0	28.8	74.7	1.595	1.597	200	(1b)
SDSSJ1418+2441	*4.50	2.8	20.9	32.8	0.572	0.573	100	(1b)
SDSSJ1426+0719	4.27	3.2	25.6	59.5	1.312	1.309	400	(1b)
SDSSJ1458+5448	5.14	65.6	31.1	90.2	1.913	1.912	0	(1b)
SDSSJ1507+2903	4.35	14.4	23.8	44.3	0.875?	0.862?	2100	(1d)
SDSSJ1530+5304	4.11	7.2	24.9	63.1	1.531	1.533	200	(2)
SDSSJ1635+2911	*4.92	25.6	29.9	77.3	1.582	1.590	900	(1b)

NOTE. — The DR4 KDE binary quasar candidate sample is now spectroscopically complete for component separations  $3.9'' < \Delta\theta < 5.2''$  for  $g < 20.85$  in regions with Galactic absorption  $A_g < 0.17$ . 20 pairs meet these criteria, and 8 of them are (the listed) binary quasars. A \* denotes a possible lens (see note in Table 1b).  $R_{prop}$  ( $R$ ) is the transverse proper (comoving) separation ( $h^{-1}$  kpc).  $|\Delta v_{\parallel}|$  is the line-of-sight velocity difference ( $\text{km s}^{-1}$ ). The final column “Table” denotes where we first listed these binaries. The 5 listed binaries with transverse separations of  $23.7 \leq R_{prop} \leq 29.9$  represent a spatially complete subsample for redshifts of  $1.03 < z < 2.10$ .